UDK 691.714:621.78.019.84
Original scientific article/Izvirni znanstveni članek

ISSN 1580-2949
Mater. Tehnol.

STUDY OF GRAPHENE COATING EFFECTIVENESS FOR MITIGATING LOW-TEMPERATURE HOT CORROSION IN SS630 STAINLESS STEEL

ŠTUDIJ UČINKOVITOSTI GRAFENSKE PREVLEKE ZA UBLAŽITEV NIZKOTEMPERATURNE VROČE KOROZIJE NERJAVNIH JEKEL VRSTE SS630

K. Amuthalakshmi[1], K. Sundaramurthy[2*], M. Makesh[2], B. K. Gnanavel[3]

[1]Department of Mechanical Engineering, Paavai Engineering College, Namakkal, Tamil Nadu, India
[2]Research Scholar, Department of Mechanical Engineering, Paavai Engineering College, Namakkal, Tamil Nadu, India
[2]Centre of Excellence for Electronic Cooling and CFD Simulation Laboratory, College of Engineering and Technology, SRM Institute of Science and Technology, Tamil Nadu, India

Prejem rokopisa – received: 2025-09-08; sprejem za objavo – accepted for publication: 2025-11-27

doi:10.17222/mit.2025.1543

In this work, the hot corrosion behavior of stainless steel 630 (17-4 PH) with and without a graphene nanoplatelet covering is examined during cyclic thermal exposure in both salt-free and salt-laden conditions. Prior to testing, SS 630 specimens were selected due to their exceptional strength and resistance to corrosion and were ultrasonically cleaned, mirror polished and precisely machined. To improve adhesion, a controlled dip coating method was used to apply a stable graphene dispersion made in ethanol, which was then thermally cured. A 1:1 combination of sodium sulfate (Na_2SO_4) and vanadium pentoxide (V_2O_5) was utilized to mimic harsh combustion conditions for salt exposure. Three temperatures, 300, 350 and 400 °C, were used for hot corrosion testing with 50 heat cycles per condition. Surface analysis and weight increase measures were used to gauge the extent of deterioration. The findings showed that corrosion rose with temperature, particularly when exposed to salt. The largest weight gain for uncoated specimens in a salt environment was 0.32 g/cm^2 at 400 °C. This was considerably lessened by graphene coverings, which decreased the weight growth by up to 52 % in salt-free and 45.6 % in salt-rich environments. Graphene-coated specimens consistently showed 40–55 % less weight increase than uncoated ones across all test conditions, according to comparative analysis. SEM examination confirmed that coated samples had better surface integrity, less oxide spallation, and less scale formation. These results demonstrate graphene's promise as a strong corrosion barrier for applications involving low temperatures. According to the study, components in heat exchangers, boilers, low-pressure stream turbines and other industrial systems subjected to corrosive and thermal stressors might have their service lives greatly increased by graphene coatings.

Keywords: graphene, hot corrosion, coatings, oxides

Avtorji v članku opisujejo raziskavo vroče korozije nerjavnega jekla vrste SS 630 (17-4 PH) brez prevleke in s prevleko iz grafenskih nanoploščic med njuno ciklično termično obremenitvijo v slanem in nesoljenem okolju. Pred testiranjem so SS 630 preizkušance, ki imajo izredno visoko trdnost in odpornost proti koroziji, očistili z ultrazvokom, mehansko obdelali in njihovo površino zrcalno spolirali. Da bi izboljšali adhezijo površine preizkušancev so avtorji izbrali metodo kontroliranega globokega potapljanja v stabilni termično obdelani disperziji grafena. Z mešanico med natrijevim sulfatom (Na_2SO_4) in vanadijevim pentoksidom (V_2O_5) v razmerju 1:1 so simulirali oziroma posnemali ostre pogoje zgorevanja. Avtorji so za preizkuse izbrali tri temperature vročega korozijskega testiranja in sicer: 300 °C, 350 °C in 400 °C s po 50 vročimi cikli. Izvedene površinske analize in meritve prirastka na masi so potrdile naraščanje stopnje poškodb. Analize so pokazale, da se stopnja korozije povečuje z naraščanjem temperature, še posobej pri vzorcih, ki so bili izpostavljeni slanemu okolju. Največji prirastek na masi 0,32 g/cm² so imeli neprevlečeni vzorci v slanem okolju pri 400 °C. Prirastek na masi se je drastično zmanjšal pri vzorcih prevlečenih z grafenom in sicer do 52 % v neslanem okolju in do 45,6 % v s soljo bogatem okolju. Primerjalna analiza je pokazala, da so imeli z grafenom prevlečeni preizkušanci, pri vseh pogojih preizkušanja, sistematično od 40 % do 55 % manjši prirastek na masi kot neprevlečeni preizkušanci. Preiskave pod vrstičnim elektronskim mikroskopom (SEM) so potrdile, da imajo vzorci z grafensko prevleko boljšo površinsko integriteto, in da je prišlo do nastanka tanjše oksidne plasti (škaje) ter manjšega luščenje oksidov. Rezultati te raziskave so pokazali, da nanoploščice grafena predstavljajo močno korozijsko bariero in tako se lahko obeta večja uporabnost grafenskih prevlek za nizkotemperaturne aplikacije kot so komponente toplotnih izmenjevalcev, bojlerjev, nizkotlačnih turbin in drugih komponent industrijskih sistemov, ki so istočasno izpostavljeni termičnim in napetostnim obremenitvam.

Ključne besede: grafen, vroča korozija, prevleke, oksidi

1 INTRODUCTION

Materials exposed to high or low temperatures are susceptible to hot corrosion, a severe type of rapid oxidation, especially when aggressive salts like sulfates and chlorides are present. The integrity and functionality of materials used in heat exchangers, boilers, low pressure stream turbines and power plants are seriously threatened by this phenomenon. The development of improved alloys, surface treatments, and protective coatings have all been the subject of much study aimed at improving corrosion resistance. The role of microstructural design,

*Corresponding author's e-mail:
sundar3003@gmail.com (K. Sundaramurthy)

chemical composition, and protective scale formation in preventing oxidation and hot corrosion has been demonstrated by recent developments in high/low temperature corrosion studies that have investigated a range of material systems, from metal oxide and sol-gel coatings to Ni-based superalloys, Mo–Si–Ti and high entropy alloys.

Plasma sprayed coatings with complex metal oxides were applied to Ni-based superalloys and tested for oxidation and hot corrosion at 800–1000 °C. The results showed that the coatings created stable oxide scales that decreased corrosion rates, although higher temperatures caused considerable scale deterioration.[1] When tested for hot corrosion at 800 °C and 900 °C for up to 100 h, two Mo–Si–Ti alloys (eutectic Mo–20Si–52.8Ti and eutectoid Mo–21Si–34Ti) demonstrated significantly thinner corrosion layers than the eutectoid alloy, indicating superior corrosion resistance.[2] In a KCl-rich environment, a study examined long-term (up to 8000 hours) alkali-induced corrosion of FeCr and coated alloys at 600 °C: FeCrAl-based coatings formed protective inner layers, while Ni-based coatings showed the slowest oxidation in laboratory tests but performed poorly in real waste-fired boilers.[3]

Under simulated refining conditions at 200–400 °C, a study investigated the corrosion behavior of AISI 444 and AISI 304 stainless steels in heavy petroleum and the results indicated that the temperature and heating method have a significant impact on corrosion, with the steels responding differently. SEM and EDX analyses showed different oxide layer formations that are indicative of temperature dependent corrosion mechanisms.[4] Hot corrosion mechanisms in complex alloy systems were analyzed using a data-driven causal discovery methodology. By focusing on crucial process factors, the method assisted in identifying important variables and causal links that affect corrosion kinetics. The findings offered fresh perspectives for creating alloys with enhanced resistance to hot corrosion.[5] Simulations showed that high compressive stress at the inner surface causes corrosion behavior and oxygen diffusion profiles that differ significantly from wet (outer) corrosion, affecting the formation of oxide layers. The study examined internal corrosion of Zircaloy cladding in PWR fuel rods, where tight contact with UO_2 pellets at 400 °C forms oxide layers that are 5–15 μm thick.[6]

After applying a NiCoCrAlY + LaZrO multilayer coating to Inconel 738, a study tested the material's ability to withstand hot corrosion at 900 °C for 240 hours in a salt vanadium environment. Electrochemical testing of the damaged sample revealed the formation of $LaVO_4$ and a 23.8 % loss in hardness.[7] Thermogravimetric, XRD and SEM/EDS analyses showed that 7 *w*/% CNT coatings provide the best microstructural integrity with minimal porosity, strong substrate bonding, and the highest corrosion resistance over 50 cycles in a Na_2SO_4 + 60 % V_2O_5 environment. The study also examined Cr C_2–25%NiCr coatings reinforced with (3, 5 and 7) *w*/% MWCNTs on ASTM SA-213T12 boiler tubes using the HVOF method to inhibit hot corrosion at 600 °C.[8]

Type II molten (Na,K) sulfate hot corrosion caused severe degradation in single crystal superalloys, resulting in non-protective scales that were 50–500 μm thick, and a weight gain of up to 40 mg/cm^2. The necessity for low-temperature hot-corrosion-resistant coatings was highlighted by the observation of dual-layer corrosion structures with Ni(Co)O- and Al(Cr)S-rich areas, with higher-Mo alloys displaying greater damage.[9] Another investigation looked at AgCl-induced stress corrosion cracking of Ti-6246 at 500 MPa and 380 °C for 24 h and found mixed corrosion products of SnO_2 and Al_2O_3 within TiO_2 as well as metallic Ag migration along cracks. Transgranular brittle fracture was observed by fractography, with dislocation patterns indicating that the cracking process was governed by dislocation emission.[10]

MnO_2/Al_2O_3 composite coatings were applied to T22 boiler steel using sol-gel techniques and tested under simulated flue-gas conditions. The composite inhibitors dramatically reduced corrosion current densities while increasing the steel resistance to hot corrosion by generating stable protective layers.[11] By preparing alloy samples using powder metallurgy and coating them with Ni-5%SiO_2-TiO_2 composites using electro deposition, another study tackled hot corrosion in steam turbines at the Al-Mussaib Thermal Power Station. The coating thickness, surface roughness, and hardness were all improved by increasing the TiO_2 content (5, 10, 15) g/L, with the sample coated with 10 g/L TiO_2 showing the highest wear resistance and the greatest reduction in wear.[12]

A study looked at how plain and welded SS316L and SS304L corroded in a molten salt solution of 10$NaNO_3$–78KNO_3–12KCl at 600 °C for 500 h and found that welded areas lost more metal and that SS304L degraded more. Salt penetration into the alloys, selective dissolving of Fe and Cr and non-adherent corrosion products were revealed by SEM and EDS investigations.[13] The microstructure and corrosion behavior of Mg–6Zn–0.5Zr–1Nd alloys made by low-pressure die casting and extrusion at 300 °C and 400 °C were investigated in another study. The results showed that an increase in the Y content refined grains and formed I-phase (Mg_3Zn_6Y) and W-phase ($Mg_3Zn_3Y_2$), improving corrosion resistance up to 1 w/% Y due to uniform phase distribution and stable oxide film formation.[14] The corrosion behavior of API X80 steel in 1 M H_2SO_4 was assessed in relation to the concentration of Fumaria officinalis (0–6 g/L) and temperature (20–60 °C). The results indicated that the inhibitor decreased anodic and cathodic reactions through physical chemical adsorption, improving corrosion resistance, but displaying decreased efficiency at higher temperatures, with the adsorption at 40 °C following the Langmuir isotherm.[15] Oxidation studies on coated AISI 441 stainless steel samples re-

vealed better corrosion resistance as a result of improved coating stability and adherence. The creation of protective oxide layers and the extension of the service life of stainless steels in oxidizing environments were validated by surface and cross-sectional investigations.[16] Graphene nanostructures grown on copper using low-temperature electron cyclotron resonance chemical vapor deposition were shown to enhance corrosion resistance. At 400 °C, the resulting graphene-coated Cu exhibited a corrosion about ten times lower than bare Cu and the presence of tall graphene nanowalls reduced the protective effect due to their layered orientation.[17]

Advanced coatings such as $PtAl_2$ dispersed (Ni,Pt)Al exhibited superior corrosion performance and minimized rumpling due to the ζ-$PtAl_2$ phase stability and improved Al diffusion compared to traditional NiAl coatings.[18] YSZ dispersion within NiCrAlY bond coats revealed a threshold concentration beyond which corrosion resistance declined, underscoring the need for optimal oxide content.[19] Likewise, HVOF-sprayed Inconel 718–Al_2O_3 composite coatings showed the highest corrosion resistance at 10 *w*/% Al_2O_3, correlating with reduced porosity.[20] Ni–20%Cr HVOF coatings on AISI 321 steel in V_2O_5–Na_2SO_4 environments demonstrated the formation of NiO, $NiCr_2O_4$, and Cr_2O_3 layers, improving resistance to oxide spallation.[21] Nano-YSZ-reinforced Ni–20Cr coatings on T22 steel showed a markedly lower weight gain in cyclic corrosion, affirming the benefit of nanoparticle reinforcement in prolonging component life.[22]

Alkali sulfate-induced hot corrosion in gas turbines persists under low sulfur fuels due to compounds like molten sodium chromate, which alter oxidation pathways and promote spinel layer growth.[23] Hot corrosion caused by a solid state process without liquid formation was recorded in single-crystal nickel-based superalloys at temperatures as low as 550 °C. Under SO_2 atmospheres, a new metastable molecule called $Na_2Ni_2SO_5$ was created. It enhanced the transport of nickel and broke down into porous NiO with embedded Na_2SO_4.[24]

Only a limited number of studies have been conducted on low-temperature hot corrosion. The problem of preventing low-temperature hot corrosion still exists where traditional oxide scales break down quickly. Recently, graphene, a two-dimensional carbon nanomaterial with remarkable chemical and thermal stability, has gained attention as a potential corrosion-resistant coating material. It may be useful in creating a barrier layer against hot corrosion because of its excellent adhesion, resistance to chemical assault and impermeability to gases and ions. This study assesses how graphene coatings can lessen the weight gain and surface deterioration of stainless steel substrates exposed to hot corrosion conditions at low temperatures.

2 EXPERIMENTAL PART

The material chosen for this investigation is stainless steel 630, often known as 17-4 PH (precipitation hardening) stainless steel. This alloy is well known for its exceptional combination of high strength, corrosion resistance, and mechanical properties, making it an ideal choice for demanding applications such as low-pressure steam turbine blades, aerospace components, and structural parts in marine and nuclear environments.

The base metal was procured in bulk and machined into flat rectangular specimens with dimensions of (20 × 10 × 3) mm. A precision cutting machine was used to assure dimensional correctness and consistency across all samples. Prior to testing, the specimens underwent a systematic surface preparation to achieve a clean, defect-free surface appropriate for examination. The specimens were initially degreased using acetone to eliminate any surface oils or impurities. To obtain a flat and smooth surface, mechanical grinding was performed using silicon carbide (SiC) abrasive sheets with successively finer grit sizes ranging from 220 to 1200 grit. To produce a mirror-like quality, final polishing was conducted using alumina slurry on a revolving polishing cloth. This procedure minimizes surface roughness, which is essential for accurate corrosion and metallurgical investigation. After polishing, the samples were ultrasonically cleaned in ethanol and dried in warm air to prevent oxidation before being further treated or tested. This meticulous preparation ensures that the surface condition of the specimens has no effect on the test outcomes, enabling reliable, reproducible research.

A stable graphene dispersion was created by dispersing high-purity graphene nanoplatelets in ethanol; it was selected for its superior wetting qualities and capacity to efficiently suspend graphene particles. The stainless steel 17-4 PH (SS 630) specimens, which had already been mirror polished and ultrasonically cleaned, were treated with ethanol to ensure full elimination of surface impurities and promote coating adhesion. To prevent agglomeration, the dispersion was ultrasonically treated for 60 min to make sure that the graphene was distributed uniformly. The withdrawal speed is a significant characteristic that directly influences the film thickness. To avoid turbulence and bubble formation, each specimen was gradually immersed into the graphene dispersion at a constant speed of 1 mm/s. The specimens were immersed in the dispersion for 5 min to ensure adequate interaction between the surface and the graphene particles. The specimens were removed vertically at a consistent rate to control the thickness of the deposited graphene. Following withdrawal, the coated specimens were air dried at room temperature to allow the solvent to evaporate. The graphene layer was then thermally cured in a hot-air oven at 80 °C for 1 h to improve adhesion and eliminate any remaining solvents.

To replicate a salt-rich environment for hot corrosion testing, the corrosive medium was a mixture of vanadium

pentoxide (V_2O_5) and sodium sulfate (Na_2SO_4). The salt combination was applied as the surface coating to the stainless steel 17-4 PH (SS 630) specimens after the operation. High-purity vanadium pentoxide (V_2O_5) and sodium sulfate (Na_2SO_4) were weighed in identical proportions (1:1). The salts were thoroughly combined with an agate mortar and pestle to create a homogeneous and fine powder combination. The produced salt combination was mixed with distilled water to form a homogenous slurry. The slurry content was kept constant to achieve a proper coating coverage, usually with approximately 20 *w*/% salt in the solvent. To prevent salt particles from settling, the slurry was churned continually. To improve salt adhesion, the mirror polished and cleaned SS 630 specimens were warmed to approximately 50 °C. The specimens were then rubbed with the salt slurry to ensure even coating on both sides of the specimen surface. After coating, the specimens were air-dried at ambient temperature for about 30 minutes to allow the solvent to evaporate. The dried, salt-coated specimens were then heated in a hot-air oven at 80 °C for 1 h to ensure that the salt layer was completely dried and adhered. This approach simulates a low-temperature corrosive atmosphere commonly observed in combustion situations, where molten salt deposits hasten the corrosion of metallic components.

Hot corrosion tests were carried out on stainless steel 17-4 PH (SS 630) specimens to determine their oxidation behavior under cyclic thermal exposure. Both uncoated and graphene-coated samples were tested in a horizontal tube furnace, with weight gain acting as the key parameter for determining corrosion severity. Specimens were ground, washed with acetone, dried, and weighed using a digital scale with a precision of 1 mg before testing. Each specimen was placed into a high purity alumina boat and fed into a preheated tube furnace with atmospheric air.

The experiment was conducted in two stages at three different temperatures: (300, 350 and 400) °C. The chosen temperature range (300–400 °C) represents the low-temperature hot corrosion regime typically encountered in components such as low-pressure steam turbine blades, marine structures, and combustion environments where salts like Na_2SO_4 and V_2O_5 may form deposits. These temperatures are below the melting point of the applied salts but high enough to promote accelerated oxidation and corrosion processes under cyclic heating. Evaluating corrosion resistance within this range provides practical insight into the alloy's behavior under service-relevant conditions, allowing assessment of the protective effect of graphene coatings in real-world applications.

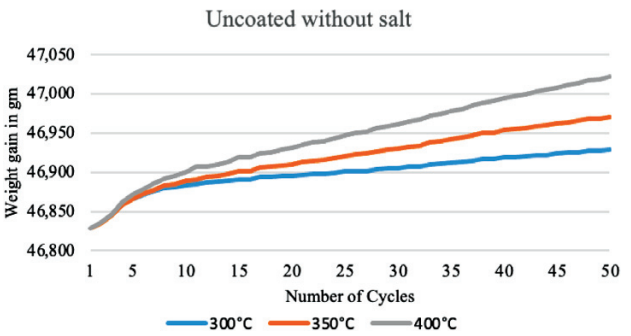

Figure 1: Weight gain of an uncoated specimen without a salt environment

Stage I – exposure without salt:

In Stage I, specimens were exposed to cyclic oxidation at predetermined temperatures without any salt layer on the surface. Each cycle included 1 hour of isothermal exposure followed by cooling to ambient temperature within a desiccator. After each cycle, specimens were weighed to determine the weight gain caused by oxide scale formation. Each temperature was cycled 50 times.

Stage II – exposure with salt:

To replicate an aggressive corrosive environment, a salt mixture of sodium sulfate (Na_2SO_4) and vanadium pentoxide (V_2O_5) was evenly applied to the specimen surfaces before each cycle. The salt-coated specimens were subjected to the same cyclic heating as in Stage I, followed by cooling and reweighing to determine corrosion-induced weight growth. Again, 50 cycles were run at each test temperature.

Throughout the stages, weight growth was the primary indicator utilized to track the deposition of oxidation and corrosion products on the specimen surfaces.

3 RESULTS AND DISCUSSION

3.1 Uncoated specimen without salt

Figure 1 shows the weight gain of an uncoated specimen during hot corrosion test without a salt environment. It depicts the oxidation behavior of the uncoated stainless steel 630 specimen subjected to cyclic thermal exposure at (300, 350 and 400) °C in the absence of salt. At 300 °C, uncoated stainless steel exhibits modest oxidation rates due to limited oxygen and metal-ion diffusion. A thin, persistent Cr_2O_3 passive coating forms to prevent further oxidation. This layer serves as a protective barrier, reducing reaction rates. Oxidation behavior begins to exhibit a parabolic pattern. At 350 °C, oxidation is more active due to enhanced ion mobility. The Cr_2O_3 layer may thicken or break down, allowing Fe_2O_3 to develop. These combined oxides offer less protection than pure Cr_2O_3. With prolonged exposure, the surface begins to degrade moderately. At 400 °C, oxygen and metal ions diffuse quickly, causing fast oxidation. Porous Fe_2O_3 dominates and replaces protective layers. The oxide scale may spall, revealing new metal repeatedly. This causes severe heat deterioration and instability. Oxidation increases with temperature and remains steady above 300 °C. At 350 °C, moderate deterioration starts with loss of passivity. At 400 °C, the large weight gain indicates inadequate oxide protection. Above 350 °C, coatings or alternative materials are necessary.

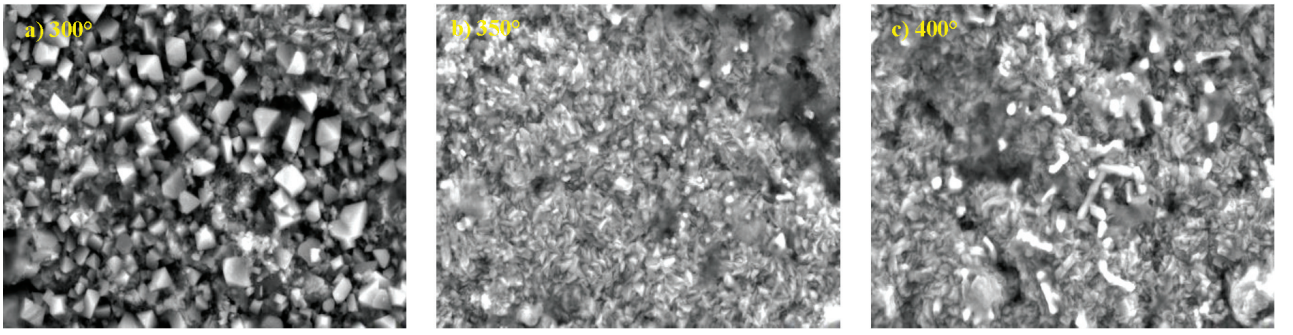

Figure 2: SEM morphology of an uncoated specimen without a salt environment

At 300 °C (**Figure 2a**), the SEM picture reveals a smooth and compact surface with well defined, angular, crystalline oxide particles. A continuous Cr_2O_3-rich layer ensures efficient protection without apparent cracks or pits. This picture shows a low corrosion activity. The weight gain of 0.101 g/cm^2 indicates negligible oxidation. At 350 °C, the surface becomes more granular and irregular, with microcracks and microscopic pits (**Figure 2b**). This indicates the onset of the Fe_2O_3 production alongside Cr_2O_3, lowering the oxide layer's protective properties. Corrosion activity is modest, and the oxide layer starts to deteriorate. The weight rise of 0.143 g/cm^2 indicates intermediate corrosion behavior. At 400 °C (**Figure 2c**), the surface appears rough, porous, and highly damaged, with huge pits and fissures throughout the oxide layer. The protective Cr_2O_3 layer is expected to break down, permitting the development of non-protective Fe_2O_3. Oxide spallation and structural breakdown are obvious. The maximum weight gain (0.194 g/cm^2) indicates significant corrosion at this stage. The weight gain data and SEM images show a clear correlation between oxidation severity and surface morphology. At 300 °C, the lowest weight gain (0.101 g/cm^2) coincides with a compact, continuous Cr_2O_3-rich layer visible in the SEM image, confirming effective passivation and minimal corrosion. At 350 °C, intermediate weight gain (0.143 g/cm^2) aligns with the SEM evidence of microcracks, pits, and mixed Cr_2O_3–Fe_2O_3 oxides, indicating the onset of protective-layer breakdown. At 400 °C, the maximum weight gain (0.194 g/cm^2) is consistent with the SEM morphology showing porous, spalled Fe_2O_3-dominated oxide layers, confirming severe corrosion and structural instability. This correlation confirms that increasing temperature accelerates oxide degradation, leading to progressively higher oxidation rates.

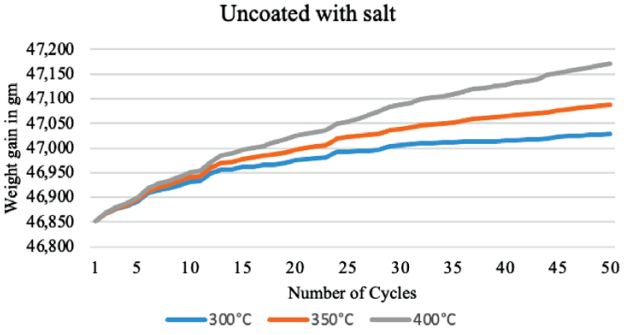

Figure 3: Weight gain of an uncoated specimen in a salt environment

3.2 Uncoated specimen with salt

The weight gain of an uncoated specimen in a salt environment is shown in **Figure 3**. The chart describes the weight gain of the uncoated material under salt exposure over 50 heat cycles at (300, 350 and 400) °C. Already at 300 °C, the presence of salt promotes oxidation relative to the absence of salt. Salt works as a flux, disrupting the Cr_2O_3 layer. This leads to quicker oxygen transport and metal ion migration. The weight gain indicates the early onset of hot corrosion. At 350 °C, with salt, the rate of oxidation accelerates dramatically. The salt promotes the breakdown of protective oxide layers, resulting in mixed, less stable oxides. Corrosion becomes more aggressive

Figure 4: SEM morphology of an uncoated specimen in a salt environment

and persistent over time. The surface begins to degrade noticeably. At 400 °C, salt significantly accelerates corrosion. A rapid formation of Fe_2O_3 and other porous oxides leads to the failure of the protective layer. Repeated spalling and oxide growth result in an ongoing weight rise. This shows that active, non-protective corrosion occurred during the test. Salt significantly accelerates corrosion at all temperatures, being the most aggressive at 400 °C. The protective behavior observed in the absence of salt is no longer present. Weight gain is increased under all conditions due to salt's catalytic impact. Thus, uncoated stainless steel without protective coatings is inappropriate for salty, high-temperature conditions.

The surface morphology of the specimen exposed to hot corrosion at 300 °C (**Figure 4a**) exhibits crisp, elongated oxide flakes, which indicate moderate oxide development. The layer appears generally intact, but it begins to show porosity and some fracturing. Formation of protective Cr_2O_3 begins, but in the presence of salt, Fe_2O_3 becomes dominant. The weight rise of 0.177 g/cm^2 indicates early corrosion activity. When exposed to 350 °C (**Figure 4b**), the oxide layer becomes increasingly fractured and uneven, with visible flake separation and surface debris. Salt accelerates oxidation, resulting in dominating Fe_2O_3 production and weakening the Cr_2O_3 layer. Small cracks and pits appear, indicating local failure and stress. The weight gain increases to 0.236 g/cm^2, indicating moderate corrosion severity. At 400 °C (**Figure 4c**), the SEM image shows a heavily corroded surface with widespread oxide spallation, huge pits, and disordered flaky Fe_2O_3 formations. The Cr_2O_3 coating is entirely disrupted, causing uncontrolled oxidation and material loss. The surface is porous and unstable, with a maximum weight gain of 0.32 g/cm^2, indicating severe hot corrosion.

3.3 Graphene-coated specimens without salt

Figure 5 depicts the hot corrosion test results for graphene-coated specimens with no salt exposure after 50 thermal cycles at (300, 350 and 400) °C. Graphene coating provides great protection at 300 °C with a minimum weight gain. The coating functions as a diffusion barrier, reducing oxygen ingress. Oxidation is reduced significantly more than in uncoated SS. The surface remains stable, and corrosion is efficiently controlled. At 350 °C, the graphene layer performs well, with slightly enhanced but controlled oxidation. The barrier remains intact, preventing mixed-oxide production. The weight gain is minimal and consistent throughout the cycles. Thermal exposure does not cause the coating to lose its integrity. The graphene layer prevents oxidation even at 400 °C, resulting in a minor increase in weight. The coating begins to exhibit signs of thermal stress, yet it still inhibits corrosion. Oxide development is more controlled than in uncoated specimens. The protective properties of graphene persist but deteriorate with temperature. The graphene covering considerably lowers oxidation at all test temperatures. It maintains a stable barrier effect up to 400 °C in salt-free conditions. Compared to uncoated stainless steel 630 specimen, the weight growth is lower and more uniform. This makes graphene a suitable surface protection material for low-temperature applications.

At 300 °C, the surface is relatively smooth as shown in **Figure 6a**, with faint polishing lines and minimum damage. There are few shallow pits, indicating that oxidation is confined and no large cracks have propagated. The graphene layer remains mostly intact and serves as a protective barrier. The low weight gain of 0.059 g/cm^2 indicates limited production of oxides like Fe_2O_3 and Cr_2O_3, demonstrating high corrosion resistance at this stage. At 350 °C (**Figure 6b**), the surface becomes rougher, with dispersed debris and micro pitting apparent throughout the sample. Slight fracture initiation is found

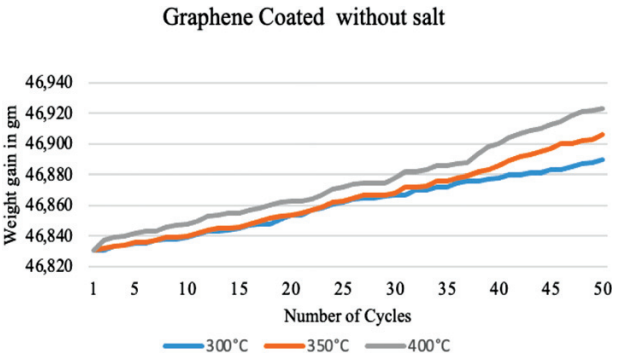

Figure 5: Weight gain of a graphene-coated specimen without a salt environment

Figure 6: SEM morphology of a graphene-coated specimen without a salt environment

along stress lines, indicating the beginning of thermal stress effects. Early stage Fe_2O_3 and Cr_2O_3 production most likely contributes to increased oxidation. The weight increment of 0.075 g/cm^2 indicates mild oxidative development, yet graphene still offers significant protection. At 400 °C (**Figure 6c**), surface deterioration occurs, including pitting, microcracks, and localized oxide clusters. The graphene layer appears to have partially broken due to thermal stress, allowing for severe oxidation. Cracks and pits allow for a deeper oxide penetration and growth, leading to an increased formation of Fe_2O_3 and Cr_2O_3. The weight gain of 0.092 g/cm^2 indicates a strong corrosion activity and oxide scale growth at high temperatures.

3.4 Graphene-coated specimens with salt

Figure 7 presents the weight gain behaviour of graphene-coated specimens in salt environment. At 300 °C, the graphene covering can successfully withstand the salt-induced corrosion. Weight gain remains low, indicating that the coating prevents salt-assisted oxidation. The protective barrier inhibits aggressive oxide production. At this stage, the material retains its great thermal and chemical stability. At 350 °C, the salt activity causes mild oxidation, but the graphene layer remains effective in preventing corrosion. Weight gain is mild and consistent across cycles. The barrier layer slows breakdown and restricts ion transfer. This specimen is more resistant than the uncoated samples. At 400 °C, salt damages the graphene coating's integrity. Although oxidation accelerates, the weight gain remains substantially lower than that of uncoated steel. The coating reduces corrosion but it may erode under heat and chemical stress. Protection remains effective, but diminished. Even when exposed to salt, the graphene coating exhibits outstanding corrosion resistance. Weight increase is consistently lower than that of uncoated specimens across all temperatures. Its barrier qualities are effective up to 350 °C and still functional at 400 °C. This indicates graphene's excellent suitability for salt-rich, high-temperature conditions.

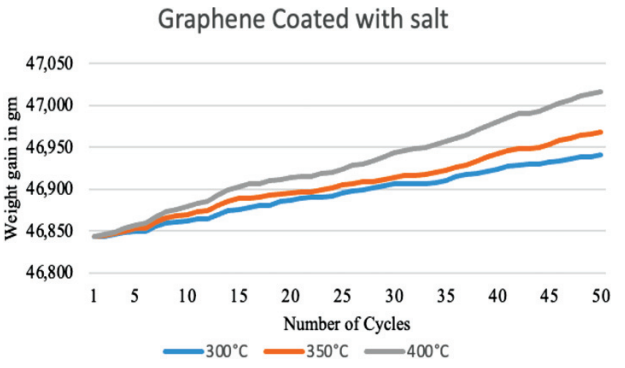

Figure 7: Weight gain of a graphene-coated specimen in a salt environment

The surface in **Figure 8a** shows early signs of deterioration at 300 °C, including superficial pitting and localized salt-induced damage. Graphene begins to degrade, exposing the substrate to corrosive substances. Minor oxide clusters, possibly Fe_2O_3, start to develop, while Cr_2O_3 patches provide partial protection. The weight gain of 0.098 g/cm^2 suggests faster corrosion owing to the salt presence compared to salt-free testing. At 350 °C (**Figure 8b**), corrosion becomes more severe, resulting in visible microcracks, deeper holes, and flake-like oxide formations. The molten salt mixture improves ion mobility, resulting in more aggressive oxidation. A thicker oxide scale containing Fe_2O_3 and Cr_2O_3 starts to build on the surface. The weight gain of 0.125 g/cm^2 indicates increasing oxidation and salt-assisted deterioration. At 400 °C (**Figure 8c**), the surface has degraded significantly, with extensive cracking, deep interconnecting pits, and dense oxide deposition. The graphene layer is substantially damaged, allowing salt components to interact intimately with the base metal. Fe_2O_3 and Cr_2O_3 scales are thick and porous, dominating the surface morphology. The weight rise of 0.174 g/cm^2 indicates hot corrosion activity and oxide buildup.

Graphene acts as a dense, inert diffusion barrier that restricts the transport of both oxygen from the atmosphere and metallic cations from the substrate. Its two-dimensional structure minimizes pathways for ionic migration, thereby slowing oxide nucleation and growth. The weight gain trends indicate that the oxidation process progresses at a much slower rate across the entire temperature range, with values increasing only slightly from 0.059 g/cm^2 at 300 °C to 0.092 g/cm^2 at 400 °C.

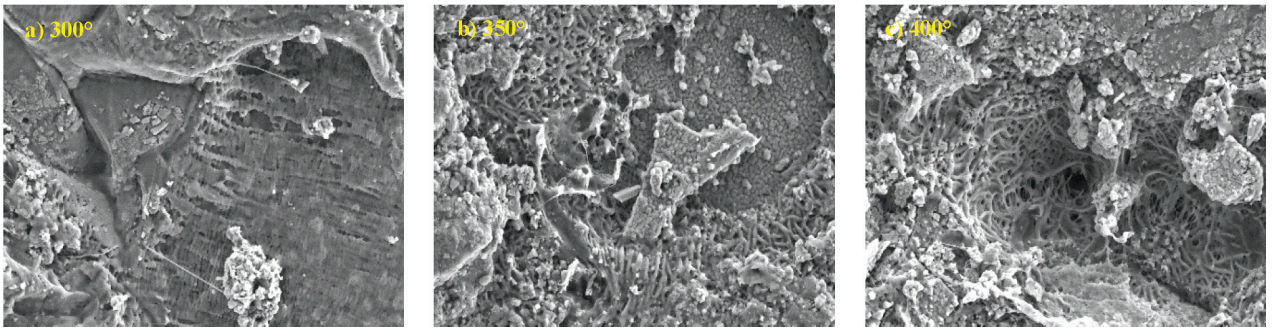

Figure 8: SEM morphology of a graphene-coated specimen in a salt environment

The steady, near-linear growth pattern suggests that the graphene coating delays the transition to parabolic oxidation kinetics typically seen in uncoated stainless steel. This indicates that the coating not only limits the oxide-scale formation but also stabilizes oxidation behavior under cyclic conditions, highlighting its potential as a high-performance surface-protection strategy.

The cyclic hot corrosion results indicate that graphene coatings primarily fail through localized degradation under combined thermal and chemical stresses. At 300 °C, the barrier remains largely intact, preventing aggressive oxidation. At 350 °C, partial breakdown occurs, evidenced by microcracks and pitting, as molten salts enhance ion mobility and promote early-stage oxide formation. By 400 °C, extensive cracking, deep pits, and thick porous Fe_2O_3/Cr_2O_3 scales indicate significant barrier compromise. These observations suggest that while graphene is highly effective at delaying corrosion, its long-term protective efficacy depends on maintaining structural integrity under thermal cycling and salt exposure. Mechanistically, protection diminishes as the coating develops defects that act as pathways for oxygen and salt ions, highlighting critical limits for high-temperature, salt-rich applications.

4 CONCLUSIONS

This study examined the hot corrosion behavior of stainless steel 630 specimens at (300, 350 and 400) °C in salt-free and salt-laden conditions, with and without graphene coatings, across 50 thermal cycles. The following important conclusions were drawn:

1. Corrosion severity increased with temperature across all situations. At 400 °C, uncoated stainless steel gained the most weight (0.32 g/cm^2) when exposed to salt. This was accompanied by severe oxide scale deposition, deep pitting, and surface degradation.

2. Salt considerably accelerates rusting. Weight gain in uncoated specimens increased by 89 % at 400 °C, indicating salt's catalytic involvement in dissolving protective Cr_2O_3 layers and increasing Fe_2O_3 production.

3. Graphene coating efficiency: Graphene-coated specimens significantly increased resistivity in salt-free conditions. At 400 °C, the weight increase decreased from 0.194 g/cm^2 (uncoated) to 0.092 g/cm^2 (coated), representing a 52 % reduction in oxidation. Graphene coatings provided substantial protection in salt environments. At 400 °C, the coated specimen gained 0.174 g/cm^2, compared to 0.32 g/cm^2 for the uncoated one. This resulted in a 45.6 % reduction in corrosion severity.

4. Comparative performance: Across all test conditions, graphene-coated samples consistently gained 40–55 % less weight than the uncoated counterparts. SEM research revealed a cleaner surface morphology, less oxide spallation, and less scale growth in coated specimens.

5. Industrial implications: The study confirms graphene's usefulness as a protective barrier for stainless steel in low-temperature corrosive conditions. Its ability to considerably decrease corrosion, even in the presence of molten salts and thermal cycling, makes it a potential material for protecting heat exchangers, boilers, low-pressure stream turbines and other low-temperature industrial components.

5 REFERENCES

[1] B. C. N. M. De Castilho, N. Sharifi, M. E. Makowiec, P. Stoyanov, C. Moreau, R. R. Chromik, Oxidation and hot corrosion behavior of multicomponent plasma-sprayed coatings on Ni-based superalloys at 800–1000 °C, J. Mater. Sci., 59 (**2024**) 23, 10508–10525, doi:10.1007/s10853-024-09787-y

[2] K. Beck, T. König, E. Senvardarli, F. Hinrichs, M. Heilmaier, M. C. Galetz, Hot corrosion behavior of Mo–Si–Ti alloys in molten salt environments, Mater. Corros., 75 (**2024**) 12, 1610–1619, doi:10.1002/maco.202414491

[3] V. Ssenteza, M. D. P. Olausson, J. Eklund, J. Nockert, J. Liske, T. Jonsson, High-temperature corrosion behavior of superheater materials at 600 °C: Insights from laboratory and field exposures, Energy Fuels, 39 (**2025**) 1, 819–827, doi:10.1021/acs.energyfuels.4c04806

[4] J. P. S. E. Machado, C. C. Silva, A. V. C. Sobral-Santiago, H. B. de Sant'Ana, J. P. Farias, Effect of temperature on the level of corrosion caused by heavy petroleum on AISI 304 and AISI 444 stainless steel, Mater. Res., 9 (**2006**) 2, 137–142, doi:10.1590/S1516-14392006000200005

[5] A. Varghese, M. Arana-Catania, S. Mori, A. Encinas-Oropesa, J. Sumner, Causal discovery to understand hot corrosion mechanisms, Mater. Corros., 75 (**2024**) 12, 1639–1651, doi:10.48550/arXiv.2402.07804

[6] J. B. Minne, L. Desgranges, V. Optasanu, N. Largenton, L. Raceanu, T. Montesin, Specific aspects of internal corrosion of nuclear clad made of Zircaloy, Defect Diffus. Forum, 323–325 (**2012**) 227–232, doi:10.4028/www.scientific.net/ddf.323-325.227

[7] A. R. Patil, S. T. Vagge, The effect of hot corrosion and electrochemical corrosion on microhardness of the coating, High Temp. Corros. Mater., 101 (**2024**), 471–483, doi:10.1007/s11085-023-10219-6

[8] M. Kuruba, G. Gaikwad, D. Shivalingappa, Hot-corrosion behaviour of CNT reinforced Cr_3C_2–NiCr coatings working under high temperature sprayed by HVOF method, Proc. Inst. Mech. Eng. Part L: J. Mater. Des. Appl., 236 (**2022**) 12, 2372–2383, doi:10.1177/14644207221082237

[9] J. L. Smialek, S. Gray, Low temperature hot corrosion screening of single crystal superalloys, Materials, 11 (**2018**) 11, 2098, doi:10.3390/ma11112098

[10] Y. Shi, S. Joseph, E. A. Saunders, R. S. Sandala, A. Walker, T. C. Lindley, D. Dye, AgCl-induced hot salt stress corrosion cracking in a titanium alloy, Mater. Sci., (2021), doi:10.48550/arXiv.2010.13875

[11] R. Chaudhary, A. Kaur, N. Bala et al., Effect of superficially applied MnO_2 and Al_2O_3 oxide inhibitors in enhancing high-temperature corrosion of T22 boiler steel, High Temp. Corros. Mater., 101 (**2024**), 703–727, doi:10.1007/s11085-024-10240-3

[12] S. Sattar, Y. Alaiwi, N. S. Radhi, Z. Al-Khafaji, O. Al-Hashimi, H. Alzahrani, Z. M. Yaseen, Corrosion reduction in steam turbine blades using nano-composite coating, J. King Saud Univ. Sci., 35 (**2023**) 8, 102861, doi:10.1016/j.jksus.2023.102861

[13] T. Joy, S. Mori, J. Sumner, High-temperature corrosion behaviour of stainless steel welds in molten $NaNO_3$–KNO_3–KCl environment for concentrated solar power, J. Energy Storage, 113 (**2025**), 115554, doi:10.1016/j.est.2025.115554

[14] H. Zengin, Y. Turen, Effect of Y addition on microstructure and corrosion behavior of extruded Mg–Zn–Nd–Zr alloy, J. Magnes. Alloys, 8 (**2020**) 3, 640–653, doi:10.1016/j.jma.2020.06.004

[15] M. Golchinvafa, S. H. Mousavi Anijdan, M. Sabzi, M. Sadeghi, The effect of natural inhibitor concentration of Fumaria officinalis and temperature on corrosion protection mechanism in API X80 pipeline steel in 1 M H_2SO_4 solution, Int. J. Press. Vessels Pip., 188 (**2020**), 104241, doi:10.1016/j.ijpvp.2020.104241

[16] D. Piel, A. Martin, E. Drouelle et al., Hot corrosion behaviour by Na_2SO_4 deposits of the 1st generation AM1 single-crystal nickel-based superalloy at 750 °C, High Temp. Corros. Mater., 101 (**2024**), 1287–1299, doi:10.1007/s11085-024-10304-4

[17] W.-H. Huang, C.-H. Lin, B.-S. Lin, C.-L. Sun, Low-temperature CVD graphene nanostructures on Cu and their corrosion properties, Materials, 11 (**2018**) 10, 1989, doi:10.3390/ma11101989

[18] Y. F. Yang, S. X. Ren, P. Ren, Q. W. Wang, Z. B. Bao, W. Li, S. L. Zhu, F. Wang, Hot corrosion and cyclic oxidation performance of a $PtAl_2$-dispersed (Ni,Pt)Al coating prepared by low-activity high-temperature aluminizing, SSRN, (**2022**), doi:10.2139/ssrn.4039448

[19] G. Sreedhar, V. S. Raja, Hot corrosion of YSZ/Al_2O_3 dispersed NiCrAlY plasma-sprayed coatings in Na_2SO_4–10 wt.% NaCl melt, Corros. Sci., 52 (**2010**) 8, 2592–2602, doi:10.1016/j.corsci.2010.04.007

[20] H. Vasudev, G. Prashar, L. Thakur, A. Bansal, Electrochemical corrosion behavior and microstructural characterization of HVOF sprayed Inconel 718–Al_2O_3 composite coatings, Surf. Rev. Lett., 29 (**2021**) 2, 2250017, doi:10.1142/S0218625X22500172

[21] S. Muthu, M. Arivarasu, B. R. Sanford, V. Dinakaran, S. Gupta, Microstructure and hot corrosion characteristics evaluation of high-velocity oxy-fuel sprayed Ni–20%Cr coating on AISI 321 steel with Na_2SO_4–60%V_2O_5 salt deposits, Proc. Inst. Mech. Eng. Part E: J. Process Mech. Eng., 238 (**2022**) 1, 299–308, doi:10.1177/09544089221143341

[22] S. Singh, K. Goyal, R. Bhatia, Molten sulphate vanadate-induced hot corrosion behaviour of YSZ-reinforced thermal spray coatings at elevated temperature, Anti-Corros. Methods Mater., 72 (**2024**) 1, 93–106, doi:10.1108/acmm-08-2024-3071

[23] C. Holländer, S. W. Kiliani, W. Stamm, O. Lüsebrink, H. Harders, E. Wessel, L. Singheiser, Hot corrosion of TBC-coated components upon combustion of low-sulfur fuels, Mater. Corros., 72 (**2021**) 10, 1643–1655, doi:10.1002/maco.202112371

[24] E. Kistler, W. Chen, G. H. Meier, B. Gleeson, A new solid-state mode of hot corrosion at temperatures below 700 °C, Mater. Corros., 70 (**2019**) 8, 1346–1359, doi:10.1002/maco.201810751